Fe-induced spin-polarized electronic states in a realistic semiconductor tunnel barrier

Massimiliano Marangolo and Fabio Finocchi
INSP, UPMC Universite Paris 06, CNRS UMR 7588, 140 rue de Lourmel, 75015 Paris, France
(Received 13 July 2007; revised manuscript received 14 January 2008; published 20 March 2008)

Whenever iron is grown on Zn-terminated ZnSe(001) substrates, the most stable configurations of Fe/ZnSe(001) magnetic tunnel junctions show Fe-Se bonding and include a Fe-Zn intermixed interface layer, as suggested by spectroscopic measurement and confirmed here by calculations based on the density functional theory. The presence of the intermixed Fe-Zn layer at the junction strongly reduces the spin polarization of both the interface and metal-induced gap states within the ZnSe tunnel barrier.

DOI: 10.1103/PhysRevB.77.115342 PACS number(s): 75.47.−m, 71.15.Mb, 73.40.Gk, 73.40.Ns

I. INTRODUCTION

Since a ferromagnetic metal (FM) provides a natural spin-polarized source, junctions between FMs and semiconductors (SCs) have been extensively studied as integrated devices for applications in spintronics.[1–3] In metal/SC interfaces, the Bloch electronic states on the metal side, with energies ranging between the SC valence band top and the Fermi energy E_F, exponentially decay in the semiconductor. Usually called metal-induced gap states (MIGS),[4] these states are usually spin-polarized in FM/SC junctions. The spatial behavior of spin-polarized MIGS is crucial in spintronics since they drive the tunneling current.[2]

Moreover, it has been shown that spin accumulation on the SC side can be obtained by means of a high enough FM/SC Schottky barrier or a tunnel barrier with a resistance comparable to that of the semiconductor,[5,6] thus remedying the resistance mismatch problem.[7] Recent experiments have also demonstrated that spin injection into the SC may be achieved and detected in a single FM/SC/FM device within a fully electrical scheme through Schottky tunnel barrier contact.[8] Furthermore, spin injection into the SC can be enhanced depending on the following characteristics of FM/SC heterojunctions: (i) a very strong spin polarization of the FM states at the interface[9] and/or (ii) spin filtering effects, which may be related to the asymmetric decay of MIGS within the SC as a function of their spin polarization.[2]

All the previous observations call for a thorough theoretical understanding of the interplay between the atomic and electronic structures of FM/SC interfaces, which can be achieved by first-principles (FP) methods.[10] However, which models must be adopted to go beyond the unrealistic case of sharp and ideal interfaces is still under debate. For instance, in Fe/MgO interfaces, FP calculations predict the spin-polarized current to be strongly dependent on the atomic structure.[11,12] Recent FP calculations of Fe/GaAs(001) and Fe/ZnSe(001) heterojunctions[13,14] showed that Fe-Zn or Fe-Ga intermixed interface-layer configurations are more stable than the ideal geometry that is usually adopted when computing spin-polarized electron transport across the junction.[2] The outcomes of the previous calculations are corroborated by high resolution transmission electron microscopy experiments,[15] by x-ray photoemission spectroscopy (XPS),[16] and by photoelectron diffraction.[17]

In this work, we consider the Fe/ZnSe(001) heterojunction, which has been experimentally and theoretically studied to such a degree that it can be considered as a prototype of low reactive FM/SC interfaces. The mismatch between bcc Fe and ZnSe is quite small (1.1%). The interface is found to be sharp without any loss of magnetic moment when iron is grown by molecular-beam epitaxy on a $c(2\times2)$ Zn-terminated ZnSe(001) surface.[18] Chemical reactivity was excluded on the basis of spectroscopic measurements even if Zn atoms are released in the Fe film and Se atoms are detected on the growth front.[16] Here, we show by first-principles calculations that the formation of an intermixed Fe-Zn monolayer with Se-Fe bonding at the interface is favored with respect to ideal heterojunctions consisting of bulk-truncated Fe and ZnSe crystals. Since the averaged transmission polarization in the generalized Jullière model[9] is indirectly linked to the interface polarization at the Fermi level and to the decay profile of polarized MIGS,[2] we analyze the influence of the structure of realistic interfacial phases on the spin polarization and on the electronic structure of the SC tunnel barrier.

II. COMPUTATIONAL DETAILS AND INTERFACE ATOMIC STRUCTURE

The calculations are carried out within the density functional theory (DFT), adopting the generalized gradient approximation[19] to the exchange and correlation energies. The projected-augmented wave representation of the Kohn–Sham orbitals is used, in conjunction with ionic pseudopotentials, as implemented in the VASP code.[20,21] The computed

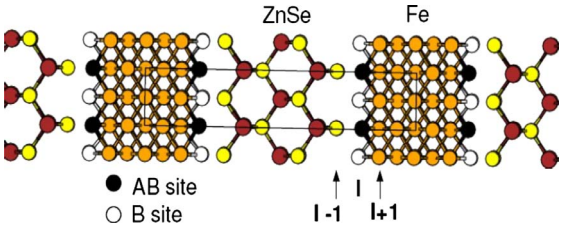

FIG. 1. (Color online) Sketch of a $(Fe2)_n/Zn_mSe_{m'}$ superlattice with the corresponding unit cell. Zn/Fe(B)Fe(AB): Zn in yellow, Se in brown, and both B and AB sites at the interface (I) occupied by Fe. Se/Fe(B)Fe(AB): as above, interchanging Zn with Se. Intermixed Se/Fe(B)Zn(AB) and Se/Zn(B)Fe(AB) configurations: Zn in brown and Se in yellow; Zn also sits at AB and B sites, respectively.

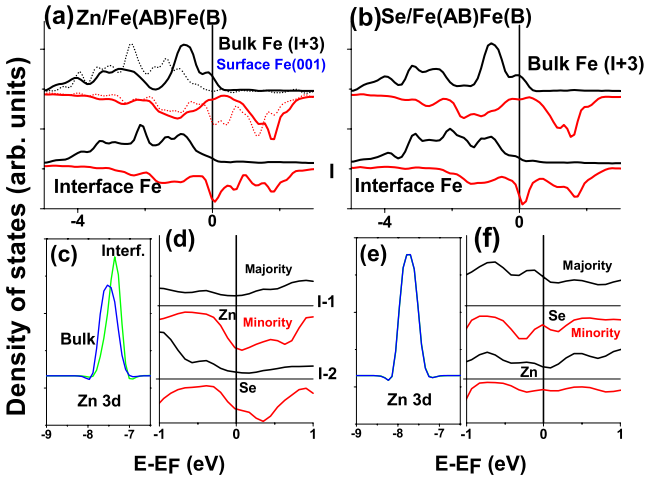

FIG. 2. (Color online) Computed LDOS of ideal interfaces: Zn/Fe(B)Fe(AB) (left) and Se/Fe(B)Fe(AB) (right). The black and red curves refer to majority- and minority-spin components, respectively. In the top (a) and (b) panels, the LDOS on the interface (I) and inner (I+3) Fe layers is drawn. (d) and (f) panels represent the behavior of MIGS through the semiconductor side, starting from the surface layer (I−1) inward. For comparison, the LDOS for the bare Fe(001) surface is given in (a). The LDOS for Zn 3d states is drawn in (c) and (e) panels.

equilibrium lattice parameters of bcc Fe and ZnSe are $a_{\mathrm{Fe}}=2.824$ Å and $a_{\mathrm{ZnSe}}=5.729$ Å, respectively; the corresponding lattice mismatch $(2a_{\mathrm{Fe}}-a_{\mathrm{ZnSe}})/a_{\mathrm{ZnSe}}$ is −1%, thus very close to +1.1%, as experimentally found. A Fermi surface smearing corresponding to 0.2 eV is adopted, with a Monkhorst–Pack sampling of the two-dimensional (2D) Brillouin zone,[22] which consists of (8,8) or (4,4) grids for the (1×1) and (2×2) 2D unit cells, respectively.

The lateral lattice parameter is always kept fixed at the theoretical value corresponding to the ZnSe substrate. Several trial configurations were built up and optimized until the residual atomic forces were less than 2 meV/Å. The local density of states (LDOS) is computed for the relaxed structures by choosing atomic spheres with radii equal to 1.27, 1.16, and 1.3 Å for Zn, Se, and Fe, respectively.

At first, we considered the deposition of n Fe monolayers on the (2×2) ZnSe(001) surface, exposing either Zn or Se, with some of them also involving Se atoms above the Fe adlayer(s). While the optimized configurations showed no symmetry but the identity at very low Fe coverage ($n\leq1$), the interfaces evolved toward more symmetrical configurations for $n>2$. Therefore, we adopted $(\mathrm{Fe2})_n/\mathrm{Zn}_m\mathrm{Se}_{m'}$ superlattices along the [001] direction, with (1×1) 2D unit cell (see Fig. 1) and $n=6$, as more effective models for the simulation of the Fe/ZnSe(001) heterojunction. They are slightly Zn rich ($m=5$ and $m=4$), which better represents the experimental conditions.[16] The $(\mathrm{Fe2})_n/\mathrm{Zn}_5\mathrm{Se}_4$ superlattices are symmetric—thus, displaying two similar junctions—and the lattice parameter along [001] is always optimized.

We find that the interface Fe/Zn monolayer stabilizes the Fe/ZnSe heterojunction in any case. In order to detail these findings, in Fig. 1, we report the ZnSe structure continued by epitaxial bcc Fe. We notice that at the interface, there are two

TABLE I. Structural parameters of the optimized interfaces: Zn/Fe(B)Fe(AB) (α), Se/Fe(B)Fe(AB) (β), Se/Zn(B)Fe(AB) (γ), and Se/Fe(B)Zn(AB) (δ). $z_{\mathrm{I}}^{(X)}-z_J$ is the vertical distance of (X) site ($X=B,AB$) from the layer beneath.

	(α)	(β)	(γ)	(δ)
$z_{\mathrm{I}}^{(AB)}-z_{\mathrm{I}-1}$ (Å)	1.56	1.68	2.04	1.86
$z_{\mathrm{I}}^{(B)}-z_{\mathrm{I}-1}$ (Å)	1.67	1.61	1.78	1.91
$z_{\mathrm{I}-1}-z_{\mathrm{I}-2}$ (Å)	1.50	1.53	1.55	1.58

nonequivalent Fe sites within the (001) planes: Half of them coincides with those of the zinc-blende crystal (B sites) and the other half corresponds to interstitials (AB sites). However, beyond the ideal case of atomically sharp Fe/ZnSe(001) junctions, AB or B sites can, in principle, be occupied by Zn or Se atoms, too. Therefore, several configurations have been simulated and four of them have been retained according to their relative stability. The corresponding junctions are Se/Fe(B)Fe(AB), Zn/Fe(B)Fe(AB), Se/Fe(B)Zn(AB), and Se/Zn(B)Fe(AB). The former two display ideal interfaces between Se- or Zn-terminated ZnSe(001) (1×1) slabs and bcc-Fe, while the latter two contain an intermixed Fe-Zn buffer layer between Se-terminated ZnSe(001) and bulk iron.

The atomic relaxations are reported in Table I for the four configurations. The intermixed Se/Fe(B)Zn(AB) and Se/Zn(B)Fe(AB) configurations are more stable than Se/Fe(B)Fe(AB) and Zn/Fe(B)Fe(AB) by 0.77 and 0.85 eV per surface (1×1) unit cell, i.e., about 0.2 J/m^2 for each of the two interfaces.[23] Substitution of Fe atoms with Zn at B or AB sites in layers that are far from the interface results in an increase of the total energy, which is consistent with the metastability of Zn-Fe alloys.[24] The formation of a mixed Zn-Fe buffer layer is thus a genuine consequence of the

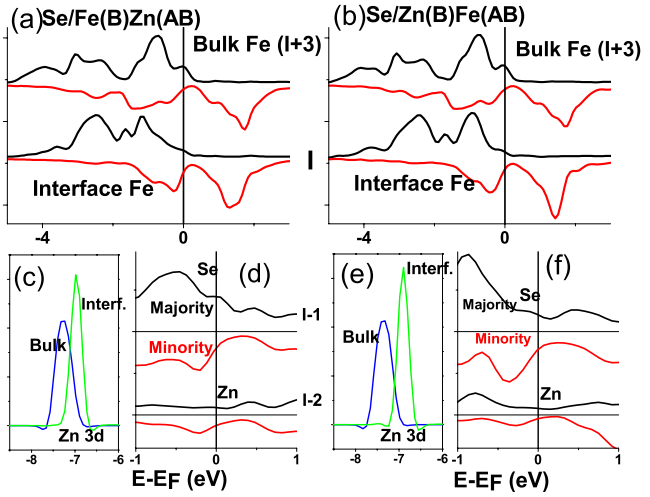

FIG. 3. (Color online) Computed LDOS of interfaces with an intermixed Zn-Se monolayer: Se/Fe(B)Zn(AB) (left) and Se/Zn(B)Fe(AB) (right). Same conventions as in Fig. 2.

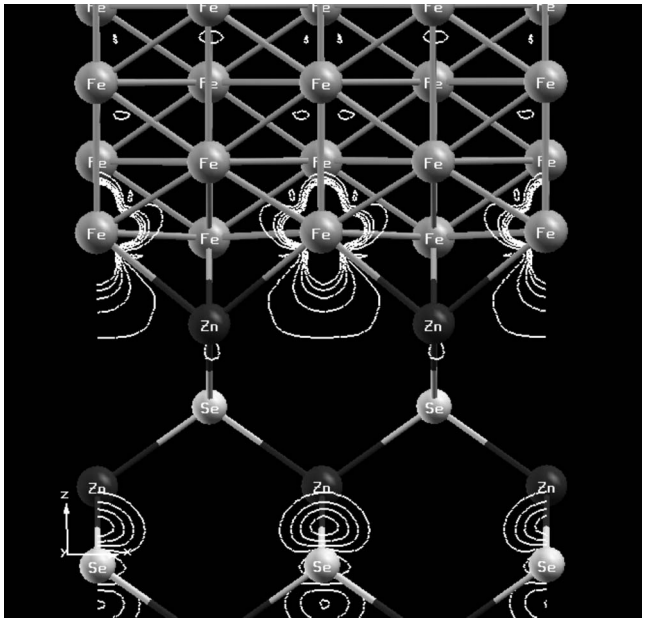

(a)

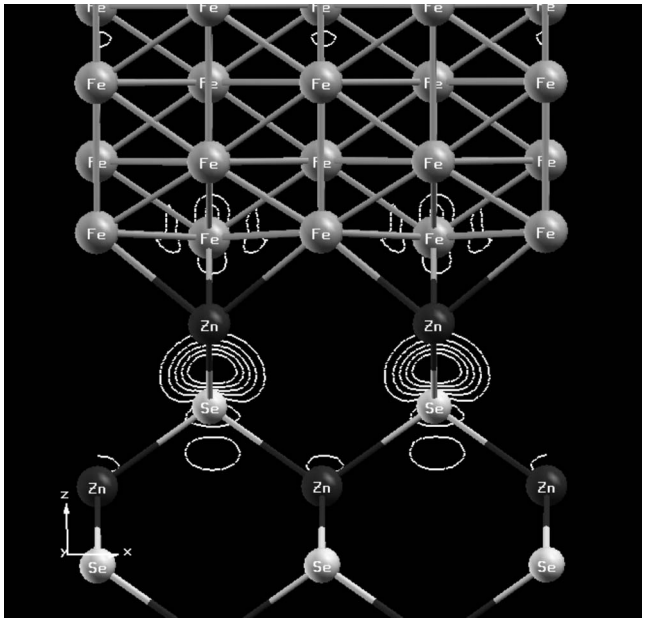

(b)

FIG. 4. Ideal Zn/Fe(B)Fe(AB) interface. Charge density plot of states at the Γ point of the minority-spin interfacial state found at the Fermi level. View along planes containing B (a) and AB (b) positions of interface Fe atoms. The isolines are drawn for minimum and maximum amplitudes of the squared wave function corresponding to 0 and 1, respectively, with interline spacing equal to 0.2 e/unit volume.

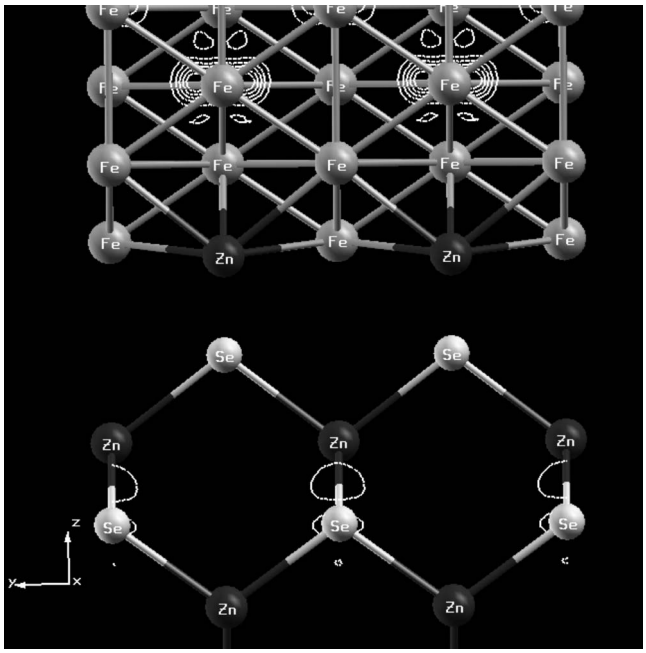

(a)

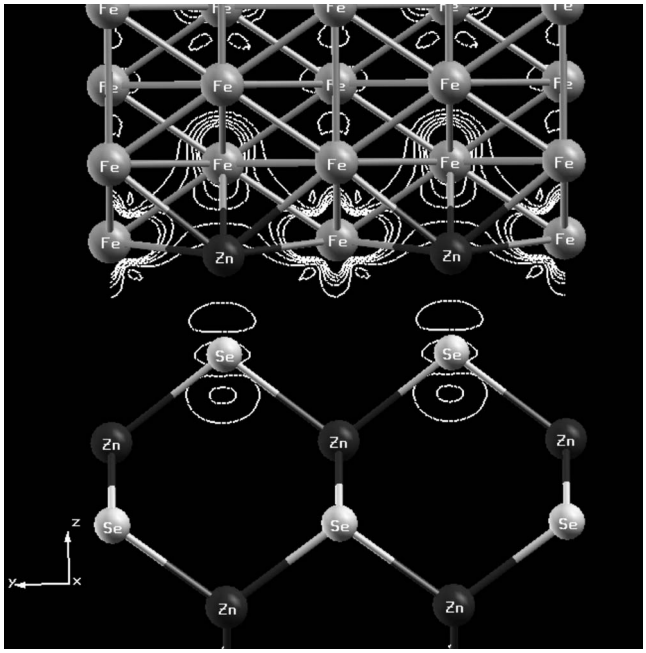

(b)

FIG. 5. Intermixed Se/Zn(B)Fe(AB) interface configuration. Charge density plot of states at the Γ point of the interfacial electronic state at ~−0.5 eV along planes containing B (a) and AB (b) sites. Same conventions for isolines as in Fig. 4.

constitution of the interface in thermodynamic equilibrium. Intermixed interfaces have also been obtained in previous DFT calculations,[14] where supercells that contain void space and stoichiometric ZnSe slabs have been used. In all cases, the interface Fe magnetic moment is enhanced by about $0.3-0.5\mu_B$ with respect to the bulk.

III. ELECTRONIC STRUCTURE: RESULTS AND DISCUSSION

The electronic density of states (DOS) of ideal and intermixed heterojunctions is calculated using a $(32\times32\times4)$ k-point grid and a Fermi surface smearing of 0.2 eV.[25] The results are shown in Figs. 2 and 3. First of all, we point out two main features: (i) close to the Fermi level, the minority-spin states dominate at the interface of the ideal heterojunc-

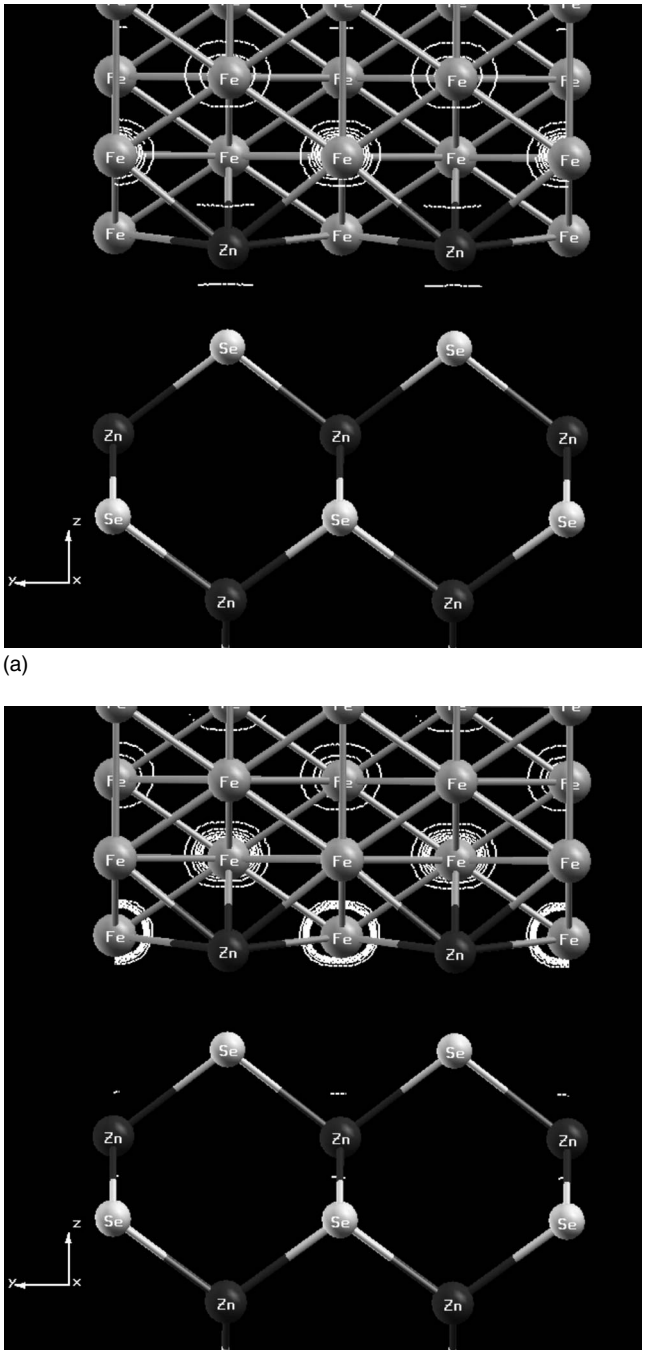

FIG. 6. Intermixed Se/Zn(B)Fe(AB) interface configuration. Charge density plot of states at the Γ point of the interfacial electronic state at ~1 eV along planes containing B (a) and AB (b) sites. Same conventions for isolines as in Fig. 4.

tions, leading to a stronger spin polarization than in the intermixed interfaces [compare Figs. 2(a) and 2(b) to Figs. 3(a) and 3(b)]; and (ii) the amplitude of the MIGS polarization within the semiconductor strongly depends on the interface geometry [compare Figs. 3(d) and 3(f) to Figs. 2(d) and 2(f)]. A more detailed report of the characteristics of the electronic structures for the four models of Fe-ZnSe heterojunctions is given below.

Regarding occupied states with Se and Zn character, our simulations allow recent XPS data[16] to be unambiguously interpreted on the basis of a microscopic model. The analysis of Se and Zn 3d chemical shifts[16] showed structural changes upon iron deposition: (i) despite the fact that Fe is grown on a Zn-terminated ZnSe(001) surface, Fe binds to Se; and (ii) some Zn atoms are reduced with respect to those in the ZnSe substrate, which has been considered as a signature of the formation of mixed ZnFe layers at the interface. Both intermixed Se/Fe(B)Zn(AB) and Se/Zn(B)Fe(AB) configurations are fully consistent with those findings; in particular, the peak corresponding to shallow Zn 3d core levels is shifted toward higher energies by about 0.5 eV with respect to ideal interfaces—compare Figs. 2(c) and 2(e) to Figs. 3(c) and 3(e)—as a result of the partial reduction of Zn atoms in passing from the substrate to the intermixed layer.

In the ideal Zn/Fe(B)Fe(AB) junction, the absolute spin polarization close to E_F is reversed with respect to bulk Fe [see Fig. 2(a)]. The Fermi level lies well above the broad structure given by a majority spin and crosses a minority-spin peak. The interface DOS of the ideal Zn/Fe(B)Fe(AB) junction is most similar to that of the bare Fe(001) surface, which is also shown in Fig. 2(a). From a comparison of the charge density plot of the minority-spin interfacial state found at the Fermi level in Fig. 4 with the surface state of Fe(001) reported by Stroscio *et al.*,[26] we conclude that the minority-spin peak at E_F is due to the d-like dangling bond of the Fe surface. The computed interface polarization at E_F is −80%. In the case of Fe/GaAs (Ref. 27) and Fe/MgO (Ref. 28) junctions, those interface states lead to a significant minority-spin polarization of the DOS at the Fermi level, and spill over into the barrier, providing a channel for the tunneling of minority spins. We notice that in the ideal Zn/Fe(B)Fe(AB) junction, MIGS-induced charge density is found on the semiconductor side, as shown in Fig. 2(d).

With respect to the Zn/Fe(B)Fe(AB) model in the ideal Se/Fe(B)Fe(AB) junction, the majority-spin peak close to E_F is broadened and its tail crosses the Fermi level. As a consequence, the overall interface spin polarization is slightly diminished (−70%). Those effects are mainly due to the Fe 3d state hybridization with Se valence orbitals. As originally pointed out by Freyss *et al.*,[29] Fe-Se bonding also affects the net spin polarization of MIGS inside the ZnSe barrier, as can be observed by comparing Fig. 2(d) to Fig. 2(f).

The presence of a Zn-Fe layer in the intermixed Se/Zn(B)Fe(AB) and Se/Fe(B)Zn(AB) interfaces induces significant modifications on the electronic structure: E_F lies in a minority-spin pseudogap [see Figs. 3(a) and 3(b)] and the interface spin polarization decreases to about −25%. In order to understand the influence of the intermixed Zn-Fe interface layer on the electronic structure, we carried out a careful analysis of the MIGS for Fe-ZnSe intermixed heterojunctions, which is partially reported below. On the basis of the spatial dispersion of the electronic states close to the Fermi level, two minority-spin states at ~−0.5 and ~1.0 eV with respect to E_F present a clear interfacial character. The corresponding charge densities are plotted in Figs. 5 and 6. Even if those states are mainly localized around interface Fe atoms, they present a resonant character with electronic bulk states. Consequently, they can play an important role in mag-

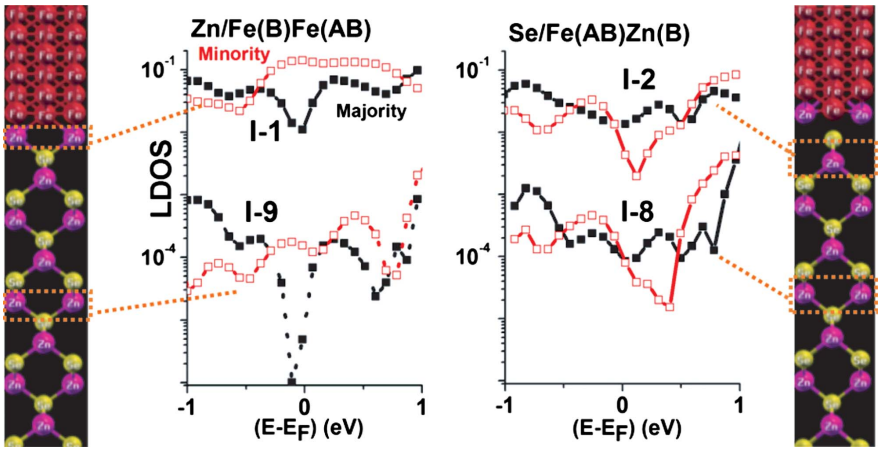

FIG. 7. (Color online) Local density of states at the Fermi energy within the ZnSe substrate as a function of the distance from the interface. Ideal $(Fe2)_7/Zn_9Se_8$ (left) and intermixed $(Fe2)_6/Zn_9Se_8$ (right) interfaces. The semilogarithmic scale evidences the exponential decay of the spin-up (full symbols) and spin-down (open symbols) MIGS within the semiconductor.

netotransport, as reported in Ref. 30. Strong modifications with respect to the ideal Fe/Zn interface (Fig. 4) can also be noticed: (i) the localization of the MIGS at −0.5 eV for the Se/Zn(*B*)Fe(*AB*) junction on the SC side (Fig. 5) is much weaker than that of the MIGS of the ideal Zn/Fe(*B*)Fe(*AB*) interface (Fig. 4), and (ii) Zn atoms essentially do not participate in the interface electronic charge redistribution around the Fermi level (Figs. 5 and 6), which is consistent with the fact that the deeper 3*d* bands of Zn are filled.

Consequently, the more realistic Fe-Zn intermixed interface structure sensitively affects the decay behavior and the polarization of metal-induced gap states within the ZnSe barrier, as summarized in Fig. 7. Indeed, in the ideal Zn/Fe interface (Fig. 7, left), the minority-spin polarization that dominates around E_F at the interface is preserved well inside the semiconductor. At variance, the intermixed configurations (Fig. 7, right) are characterized by a lower net spin polarization, whose sign is dependent on the applied bias voltage, which is both close to the interface and more deeply into the semiconductor. Bias-dependent transmission properties through the tunnel barrier, as recently reported for CoFe/MgO tunnel junctions,[30] might thus be conceived for the intermixed Fe-ZnSe interfaces.

IV. CONCLUSIONS

In conclusion, a Fe-Zn intermixed buffer monolayer at the Fe/ZnSe(001) interface, which is predicted here to be energetically favored, dramatically affects the interface electronic structure. Both Se/Fe(*B*)Zn(*AB*) and Se/Zn(*B*)Fe(*AB*) model junctions have little negative polarization at E_F with respect to ideal Fe/ZnSe(001) interfaces. As far as spintronics is concerned, one important consequence is the strong reduction of the MIGS spin polarization inside the SC barrier since spin injection depends on the competition between the majority and minority channels. However, since in the intermixed configurations the MIGS polarization around the Fermi level is energy dependent, a majority- to minority-spin switch of the injected electrons in Fe/ZnSe/SC heterojunctions might be conceived. Nevertheless, the most favored architectures for spintronics applications are the ideal Zn/Fe or Se/Fe junctions;[31] we are currently exploring the possibility that similar interfaces could be stabilized by low-temperature growth in Zn-rich environments.

ACKNOWLEDGMENTS

Calculations were performed at the IDRIS Supercomputing Center (Orsay, France) under Project No. 061820. We thank M. Eddrief, F. Vidal, N. Jedrecy, and V. H. Etgens for useful discussions.

[1] I. Zutic, J. Fabian, and S. Das Sarma, Rev. Mod. Phys. **76**, 323 (2004).
[2] X.-G. Zhang and W. H. Butler, J. Phys.: Condens. Matter **15**, R1603 (2003); Ph. Mavropoulos, N. Papanikolaou, and P. H. Dederichs, Phys. Rev. Lett. **85**, 1088 (2000); Ph. Mavropoulos, O. Wunnicke, and P. H. Dederichs, Phys. Rev. B **66**, 024416 (2002).
[3] J.-M. George, M. Elsen, V. Garcia, H. Jaffrès, and R. Mattana, C. R. Phys. **6**, 966 (2005).
[4] V. Heine, Phys. Rev. **138**, A1689 (1965).
[5] E. I. Rashba, Phys. Rev. B **62**, R16267 (2000).
[6] A. Fert and H. Jaffrès, Phys. Rev. B **64**, 184420 (2001).
[7] G. Schmidt, D. Ferrand, L. W. Molenkamp, A. T. Filip, and B. J. van Wees, Phys. Rev. B **62**, R4790 (2000).
[8] X. H. Lou, C. Adelmann, S. A. Crooker, E. S. Garlid, J. Zhang, K. S. M. Reddy, S. D. Flexner, C. J. Palmstrøm, and P. A. Crowell,

Nat. Phys. **3**, 197 (2007).
[9] M. Jullière, Mod. Phys. Lett. A **54**, 225 (1975).
[10] M. Peressi, N. Binggeli, and A. Baldereschi, J. Phys. D **31**, 1273 (1998).
[11] C. Tusche, H. L. Meyerheim, N. Jedrecy, G. Renaud, A. Ernst, J. Henk, P. Bruno, and J. Kirschner, Phys. Rev. Lett. **95**, 176101 (2005).
[12] Christian Heiliger, Peter Zahn, Bogdan Yu. Yavorsky, and Ingrid Mertig, Phys. Rev. B **73**, 214441 (2006).
[13] S. C. Erwin, S.-H. Lee, and M. Scheffler, Phys. Rev. B **65**, 205422 (2002).
[14] B. Sanyal and S. Mirbt, Phys. Rev. B **65**, 144435 (2002); S. Mirbt, B. Sanyal, C. Isheden, and B. Johansson, *ibid.* **67**, 155421 (2003).
[15] T. J. Zega, A. T. Hanbicki, S. C. Erwin, I. Žutić, G. Kioseoglou, C. H. Li, B. T. Jonker, and R. M. Stroud, Phys. Rev. Lett. **96**, 196101 (2006).
[16] M. Eddrief, M. Marangolo, V. H. Etgens, S. Ustaze, F. Sirotti, M. Mulazzi, G. Panaccione, D. H. Mosca, B. Lépine, and P. Schieffer, Phys. Rev. B **73**, 115315 (2006); M. Eddrief, M. Marangolo, S. Corlevi, G.-M. Guichar, V. H. Etgens, R. Mattana, D. H. Mosca, and F Sirotti, Appl. Phys. Lett. **81**, 4553 (2002).
[17] P. Schieffer, A. Guivarc'h, C. Lallaizon, B. Lépine, D. Sébilleau, P. Turban, and G. Jézéquel, Appl. Phys. Lett. **89**, 161923 (2006).
[18] M. Marangolo, F. Gustavsson, M. Eddrief, Ph. Sainctavit, V. H. Etgens, V. Cros, F. Petroff, J. M. George, P. Bencok, and N. B. Brookes, Phys. Rev. Lett. **88**, 217202 (2002).
[19] J. P. Perdew and Wang Yue, Phys. Rev. B **33**, 8800 (1986).
[20] G. Kresse and D. Joubert, Phys. Rev. B **59**, 1758 (1999).
[21] G. Kresse and J. Hafner, Phys. Rev. B **47**, 558 (1993); G. Kresse and J. Furthmüller, *ibid.* **54**, 11169 (1996).
[22] H. J. Monkhorst and J. D. Pack, Phys. Rev. B **13**, 5188 (1976).
[23] In order to compare the different model junctions directly, the total energy corresponding to Zn/Fe(B)Fe(AB) has been computed by averaging over $Fe_{10}Zn_5Se_4$ and $Fe_{14}Zn_5Se_4$ superlattices, whose interfacial structures are essentially the same.
[24] F. Zhou, Y. T. Chou, and E. J. Lavernia, J. Mater. Res. **17**, 3230 (2002).
[25] A Fermi surface smearing of 0.1 eV did not significantly modify the electronic DOS.
[26] Joseph A. Stroscio, D. T. Pierce, A. Davies, R. J. Celotta, and M. Weinert, Phys. Rev. Lett. **75**, 2960 (1995).
[27] D. O. Demchenko and A. Y. Liu, Phys. Rev. B **73**, 115332 (2006).
[28] C. Tiusan, J. Faure-Vincent, C. Bellouard, M. Hehn, E. Jouguelet, and A. Schuhl, Phys. Rev. Lett. **93**, 106602 (2004).
[29] M. Freyss, N. Papanikolaou, V. Bellini, R. Zeller, and P. H. Dederichs, Phys. Rev. B **66**, 014445 (2002).
[30] L. Gao, Xin Jiang, See-Hun Yang, J. D. Burton, Evgeny Y. Tsymbal, and Stuart S. P. Parkin, Phys. Rev. Lett. **99**, 226602 (2007).
[31] J. Peralta-Ramos and A. M. Llois, Physica B: Condensed Matter **398**, 393 (2007).